SLAC–PUB–6306
SLAC/SSRL–0042
August 1993
(A/SSRL–M)

Modern Theory and Applications of Photocathodes *

W. E. Spicer
Stanford Synchrotron Radiation Laboratory, Stanford Linear Accelerator Center, and
Stanford Electronics Laboratories, Stanford, California 94305

A. Herrera-Gómez
Stanford Linear Accelerator Center and
Stanford Electronics Laboratories, Stanford, California 94305

Abstract

Over the last thirty years, the Spicer Three–Step model has provided a very useful description of the process of photoemission for both fundamental and practical applications. By treating photoemission in terms of three successive steps—optical absorption, electron transport, and escape across the surface—this theory allows photoemission to be related to parameters of the emitter, such as the optical absorption coefficient, electron scattering mechanisms, and the height of the potential barrier at the surface. Using simple equations and established parameters, the Three–Step model predicts the performance of cathodes and provides detailed understanding of the unexpected phenomena that appear when photocathodes are pushed into new practical domains. As an example, time responses are estimated for existing cathodes, and are found to cover a range of six orders of magnitude. Further, the time response is found to be directly related to the sensitivity (i.e., quantum efficiency) of the cathode. The quantum yield systematically decreases with the time response. Thus, metals are predicted to have the shortest time response (as little as 10^{-15} sec) and the smallest quantum efficiency (as little as 10^{-4} electrons per photon), whereas the negative affinity photocathodes have high yield (as high as 0.6 electrons per photon) but long response times (as long as 10^{-9} sec). Other applications of the Three–Step model are discussed.

1. Introduction

The purpose of this article is to draw together and add to the existing material on the physics of practical photocathodes. Although Einstein received the Nobel Prize for his quantum theory of photoemission published in 1903, it took over 50 years before a comprehensive understanding of the photoemission process was obtained [1,2,3] The historic problem was that researchers tended to believe that it was a surface rather than a bulk effect [4]. Thus, the optical absorption was considered a surface (not bulk) phenomena and electron transport through the solid was not considered. This "surface photoemission" concept was reinforced by early beliefs that the electron moment could only be conserved by interacting with the surface [2,3]. In the mid–1940s, Fan [5] showed that momentum could be conserved by Bragg reflections of the electrons from the crystal planes in a crystalline solid. Later experimental work showed this to be the case for non-crystalline solids as well [6]. Fan's work showed that the excitation could be in the bulk.

In the 1950s, experimental work appeared that definitively showed that photoemission was a bulk phenomena [2,3]. In 1958, Spicer [7] developed a model or theory for photoemission, often called the Three Step Model, that for the first time treated photoemission as a bulk process—and treated it in terms of bulk optical constants and electron scattering lengths, as well as surface properties such as the position of the vacuum level (work function) at the surface of the solid. In the last 25 years, this theory has provided a means of understanding practical photoemitters. In addition, it has been found to describe photoemission from all solids. It has not only helped in the development and understanding of practical photoemitters, but in fact has also made possible the development of an important scientific tool: the photoemission spectroscopic (PES) [1,2,3]. The 1958 Three–Step model was derived to give the quantum efficiency of a photoemitter as a function of photon energy. In 1964, Berglund and Spicer [9] published a more sophisticated formalization of the Three–Step model that gives the absolute value of the distribution in energy of the photoelectrons.

For our purpose here, it is sufficient to derive the expression for quantum efficiency. This will be done in the next section. This Three–Step formalization allows us to examine much more than just the yield. We will use it to provide estimates of the response time of photoemission for various materials and to examine electron scattering effects. In a separate paper in these proceedings, Herrera-Gómez and Spicer discuss a limitation on charge than can be drawn from a cathode.

Work supported in part by Department of Energy contract DE-AC03-76SF00515 (SLAC/SSRL), and in part by the Dean of Engineering, Stanford University (W.E.S.) and by CONACyT-México (A.H.).

Presented at SPIE's 1993 International Symposium on Optics, Imaging and Instrumentation, San Diego, CA, July 11-16, 1993

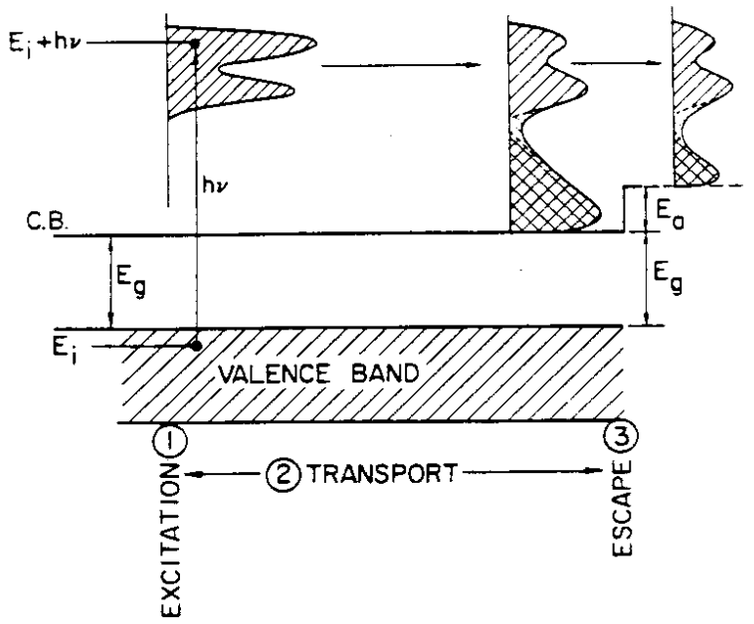

Figure 1. The three step model. The photoemission process can be divided into three steps: 1) photoexcitation, 2) transport to the surface, and 3) escape to vacuum.

2. Derivation of an Expression for Quantum Yield

Essential to the Three–Step model is the recognition that bulk absorption coefficient governs the excitation of photoelectrons. The light intensity, $I(x,h\nu)$, after it transverses a thickness x of a solid is given by

$$I(x,h\nu) = I_o(h\nu)\,[1-R(h\nu)]\;e^{-\alpha(h\nu)x}\;, \tag{1}$$

where $I_o(h\nu)$ is the incident intensity of light of photon energy $h\nu$, $R(h\nu)$ is the light reflectivity from the surface of the solid, and $\alpha(h\nu)$ is the absorption coefficient of the solid. Thus, the amount of light absorbed at a distance x from the surface is:

$$dI(x) = (1-R)\;I_o\;e^{-\alpha(h\nu)x}\;\alpha\,dx\;. \tag{2}$$

Some of the photoexcited electrons will travel to the surface and escape. The contribution $di(x)$ to the photoemission yield from excitation in the slab of thickness dx at x is given by

$$di(x) = P_{o\alpha}(h\nu,x,dx)\;P_T(h\nu,x)\;P_E(h\nu)\;, \tag{4}$$

where $P_T(h\nu,x)$ is the probability that electrons (excited by photons of energy $h\nu$ at a distance x from the surface) will reach the surface with sufficient energy to escape.

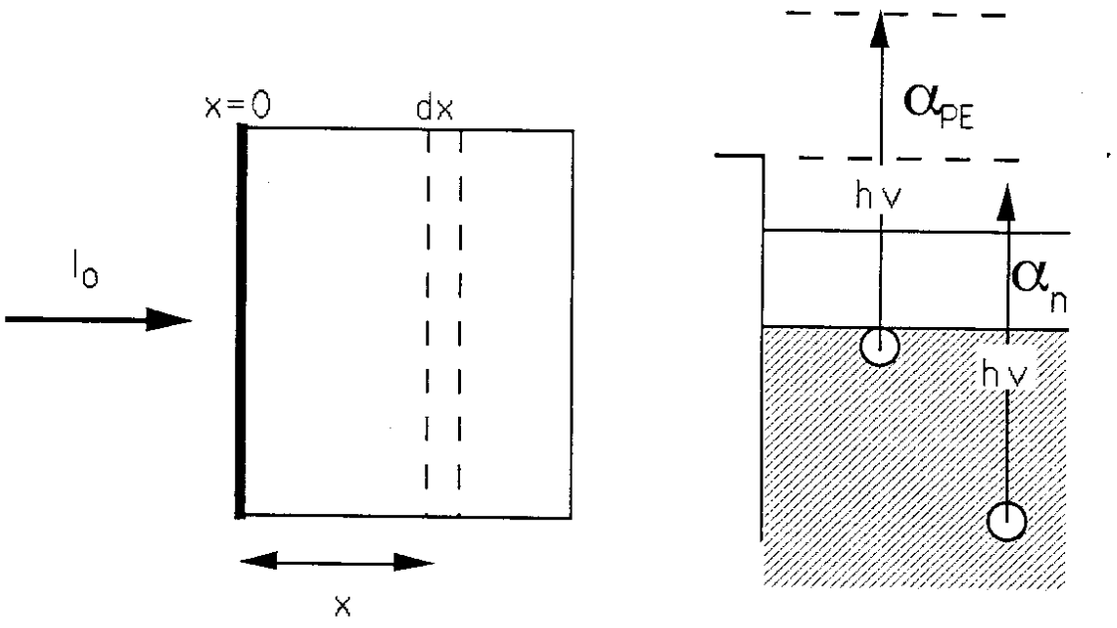

Figure 2. The contribution to the photoemission yield from excitation in the slab of thickness dx depends on the distance x from the surface, where α_{PE} represents the part of the absorption where the electrons are excited above the vacuum level and have a possibility to escape, and α_n is the absorption that does not produce any yield.

Because the scattering probability is proportional to the distance traveled, it can be shown that [7]

$$P_T(x,h\nu) = \exp\left\{-\frac{x}{L(h\nu)}\right\} . \tag{5}$$

$P_E(h\nu)$ is the probability of escape of electrons reaching surface with sufficient energy to escape. $P_{o\alpha}(h\nu,x,dx)$ is the probability of exciting electrons above Vacuum Level (VL) in the slab between x and $x+dx$, and is given by

$$P_{o\alpha}(h\nu,x,dx) = \alpha_{PE}(h\nu)\ I(x)\ dx = \alpha_{PE}(h\nu)\ I_o(1-R)\ e^{-\alpha x}\ dx . \tag{6}$$

We then have

$$di(x) = I_0(1-R)\ \alpha_{PE}\ e^{-\alpha x}\ e^{-\frac{x}{L}}\ P_E(h\nu)\ dx .$$

For a semi-infinite slab, the total electron yield is $i(h\nu) = \int_0^\infty di(x)$ then

$$i(h\nu) = I_0(1-R)\ \frac{\alpha_{PE}}{\alpha+\frac{1}{L}}\ P_E(h\nu) . \tag{7}$$

The quantum yield (QY) is defined as the number of electrons emitted per absorbed photon:

$$QY(h\nu) \equiv \frac{i(h\nu)}{I_0(1-R)} = \frac{\frac{\alpha_{PE}}{\alpha} P_E}{1+\frac{1}{\alpha L}} \quad , \tag{8a}$$

where I_0, R, α_{PE}, α, L, and P_E are all functions of $h\nu$.

This is the basic equation for photoemission quantum yield. We rewrite Eq. 8a as follows

$$QY = \frac{\frac{\alpha_{PE}}{\alpha} P_E}{1+\frac{l_a}{L}} \quad , \tag{8b}$$

where $l_a(h\nu) \equiv 1/\alpha(h\nu)$ is the absorption length, l_a/L is the ratio of absorption length to scattering length, and α_{PE}/α is the fraction of electrons excited above vacuum level

3. How the Parameters of Eq. 8 Determine the Quantum Efficiency

First examine l_a/L , the ratio of the optical absorption length, l_a, to the escape length, L. As Fig. 3 shows, if the absorption takes place over a distance large compared to the escape distance, few of the excited electrons escape and the quantum efficiency will be low.

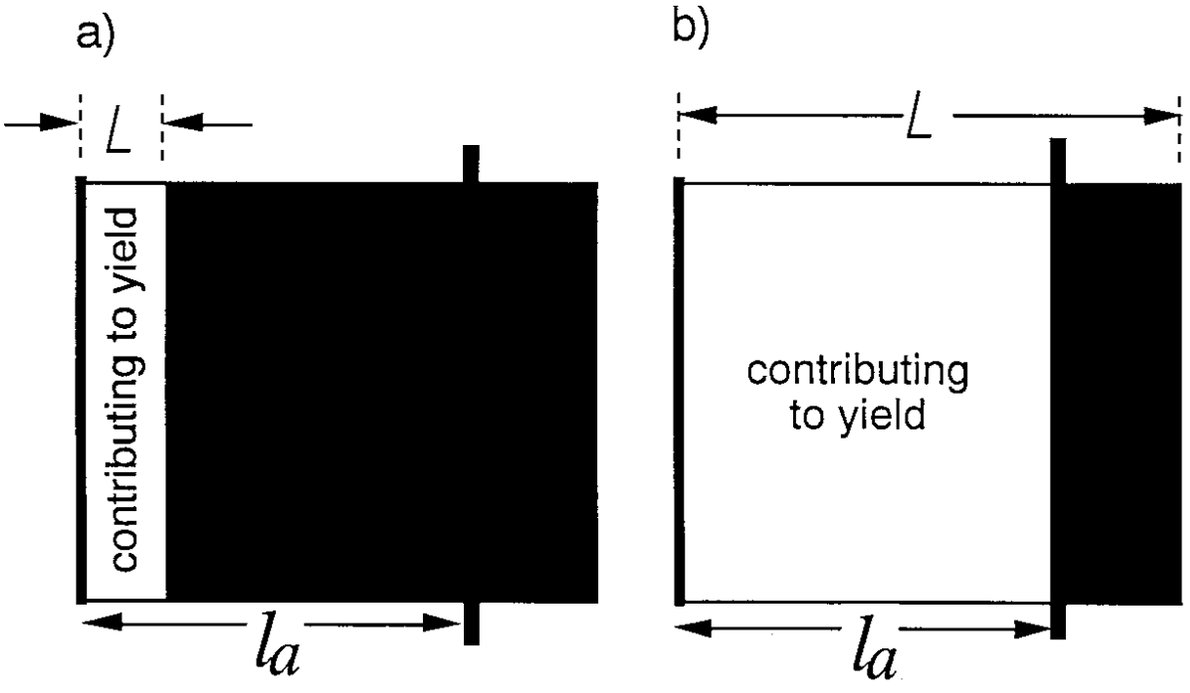

Figure 3. The white volume is the region contributing to the yield. L is the escape length, and l_a is the absorption length. If $L << l_a$, then only a small fraction of the photoexcited electron contributes to the yield.

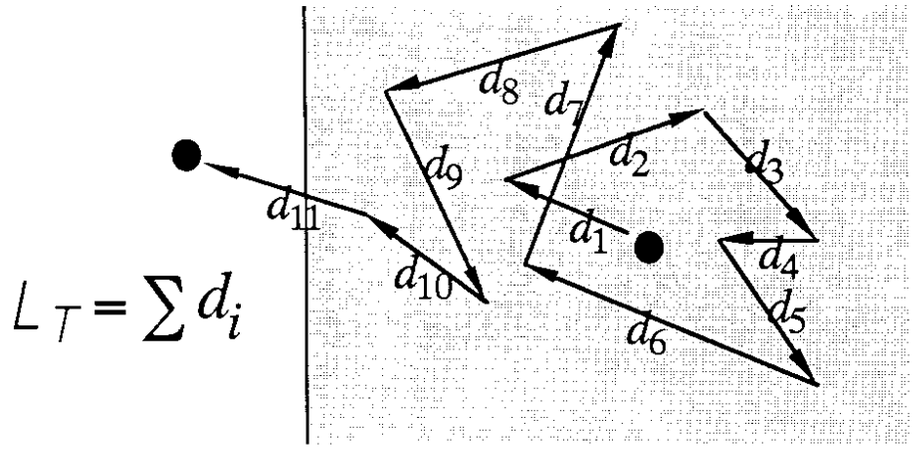

Figure 4. Transport of a photoemitted electron when the electron-phonon scattering is dominant. The integrated path, L_T, is the sum of the distances traveled between collisions.

For example, in the hard ultraviolet region ($h\nu$ ~ 60 eV), l_a/L might be as high as 10^4. For Cs metal it can be 10^3 in the near ultraviolet ($h\nu$ ~ 5 eV). Thus, the yields will be very low. However, in some semiconductors it can be close to unity in the visible or infrared. This is what makes possible the high quantum efficiency of semiconductors such as Cs_3Sb, [Cs]Na_2KSb, [7,13], and the negative affinity GaAs [15,16,17]. Large band gap insulators such as CsI (E_g ~ 6eV) [14] have high efficiencies in the ultraviolet (e.g., 10 eV) because l_a/L can be less than unity. The ratio l_a/L is often the dominant parameter determining the quantum yield since it can vary by as much as 10^4 between various materials. In order to relate l_a/L to characteristics of a given solid, we must understand the electron scattering mechanisms that determine L. This will be covered in Section 4. As will be shown in Section 5, L is important in determining the photoemission time response.

Next consider α_{PE}/α. This is simply the fraction of the electrons excited above the vacuum level. It will normally increase monotonically as $h\nu$ increases above the threshold for photoemission. Clearly α_{PE}/α will be maximized by lowering the vacuum level (VL) toward the conduction band minimum (CBM), i.e., reducing the electron affinity (E_A), which is the difference in energy between the *VL* and the bulk CBM. All efficient photoemitters have values of α_{PE}/α between 0.1 and 1.0. The negative affinity emitters (see Section 5) have an α_{PE}/α of almost unity.

The escape probability normally increases monotonically with $h\nu$. However, for the efficient alkali-antimonides (e.g., Cs_3Sb and [Cs]Na_2KSb) and negative affinity cathodes, it can be well approximated by a step function. Usually P_E does not exceed 0.5; however, in certain very favorable cases, such as CsI [14], the yield approaches 1 electron/photon thus P_E must approach unity. This can be explained by the fact that CsI has a narrow valence band so that all electrons are excited above the VL and only electron-phonon scattering must be considered, as discussed in the next section. In cases where electron-electron scattering dominates, as is the case for most metals, P_E may be below 0.1, even well away from the hreshold.

4. Electron Scattering Mechanisms and their Effect on l_a/L and Photoemission Efficiency.

The principal inelastic electron scattering mechanisms are electron-phonon (lattice) and electron-electron scattering. These mechanisms are illustrated by Figs. 4 and 5.

Because of its small energy loss per collision and the fact that the scattering tends to change the direction of motion of electrons, electron-phonon scattering—under favorable conditions—can increase the photoemission efficiency. This is because, on the average, the electrons will be excited with their momentum vectors in all directions. However, it is the momentum perpendicular to the surface that allows electrons to escape from the surface [4]. Half the excited electrons will have momentum vectors away from the surface and, near threshold, only a small fraction may have momentum close enough perpendicular to the surface to escape. However, phonon scattering changes the direction of motion of the electron and may place it in the right direction to escape. This effect will only be helpful if electron-electron scattering can be neglected.

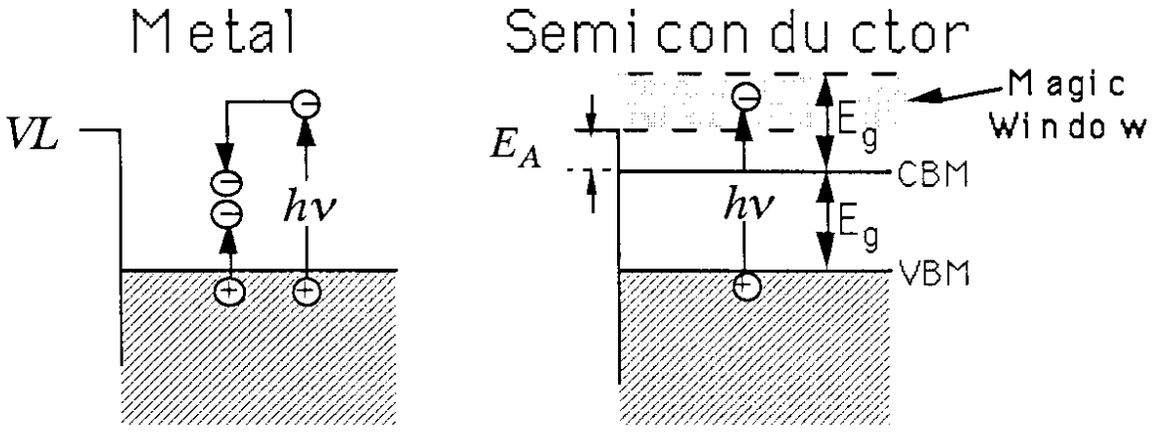

Figure 5. Comparison of electron-electron scattering in metals and semiconductors. In a metal, an electron may lose the energy needed to escape in a single electron-electron scattering event (pair production). Semiconductors can have a "Magic Window," where electrons have enough energy to escape, but not enough to produce pairs.

In order to fully appreciate this mechanism, it is useful to think of the photoemission process as a random walk (with small loss per collision) with an absolute sink at the surface for the electron escape. If there is no other loss mechanism, electrons will have many chances to escape before they lose enough energy from electron-photon scattering to fall below the VL. This is the reason why the yield from CsI can approach unity, and probably the reason why P_E can rise so sharply near threshold for the efficient alkali antimony emitters and negative affinity photocathodes (see previous section). If the average loss per lattice collision is 0.01 and the electron is excited 1.0 eV above the VL, it must suffer 100 collisions before it falls below the VL.

Figures 5 and 6 give insight into electron-electron scattering, as well as the reason why semiconductors can be much more efficient photoemitters than metals. As the left-hand panel of Figure 5 shows, the primary electrons in a metal can lose a large fraction of its energy in one scattering event. Near threshold, the increase in the energy of the secondary electron won't be enough to allow it to escape, so neither electron will be able to escape. Thus, the escape depth will be short. In a semiconductor with a sufficiently low electron affinity, there is no electron-electron scattering near threshold, and thus we have a long escape depth and the "magic window."

As Fig. 6a shows, the electron-electron scattering lengths (L_e) decrease as the electron's energy increases, and can have very small values. Figure 6 gives $L_e(E)$, the electron-electrons scattering length, as a function of electron energy for a variety of materials. Whereas $L_e(E)$ is the most fundamental way of presenting electron-electron scattering data, $L(h\nu)$ is most useful for calculating yields. $L(h\nu)$ can be obtained from $L_e(E)$ by averaging $L_e(E)$ over the distribution in energy of the electrons excited by photons of energy $h\nu$. $L(h\nu)$ can also be obtained directly from experiment. An example of this is given in Fig. 6b where the values of $L(h\nu)$ published by Spicer [18] in 1963 for [Cs]Na_2LSb are presented. Berglund and Spicer [18] and Kane [19] have calculated $L(h\nu)$ curves. Stuart et al. [20] have treated both electron-electron and electron-phonon scattering using Monte Carlo techniques.

Note that $L(h\nu)$ can be as low 10Å or less. Assuming $l_a \approx 300Å$, we see that l_a/L can be as high as 30 or more. Thus, the quantum yield of unscattered electrons will be reduced by 1/30. However, since the $h\nu$ needed to obtain such a small value of L is usually large, the scattered electrons will be above the VL so that they may escape. For $h\nu$ near the threshold for photoemission in metals, however, none of these scattered electrons will be able to escape. For metals, L near threshold can still be fairly small. For $h\nu$ an electron-volt above threshold, L is approximately 40 Å for Cu [19] and 10 Å for Cs [20] .

The difference between metals and semiconductor (and insulators) as photoemitters lies in the nature of $L(h\nu)$. For metals, any optically excited electron can suffer electron-electron scattering; for non-metals this is not the case. Since a finite band gap, E_g, separates the highest states filled with large numbers of electrons [21] and the lowest conduction band states,

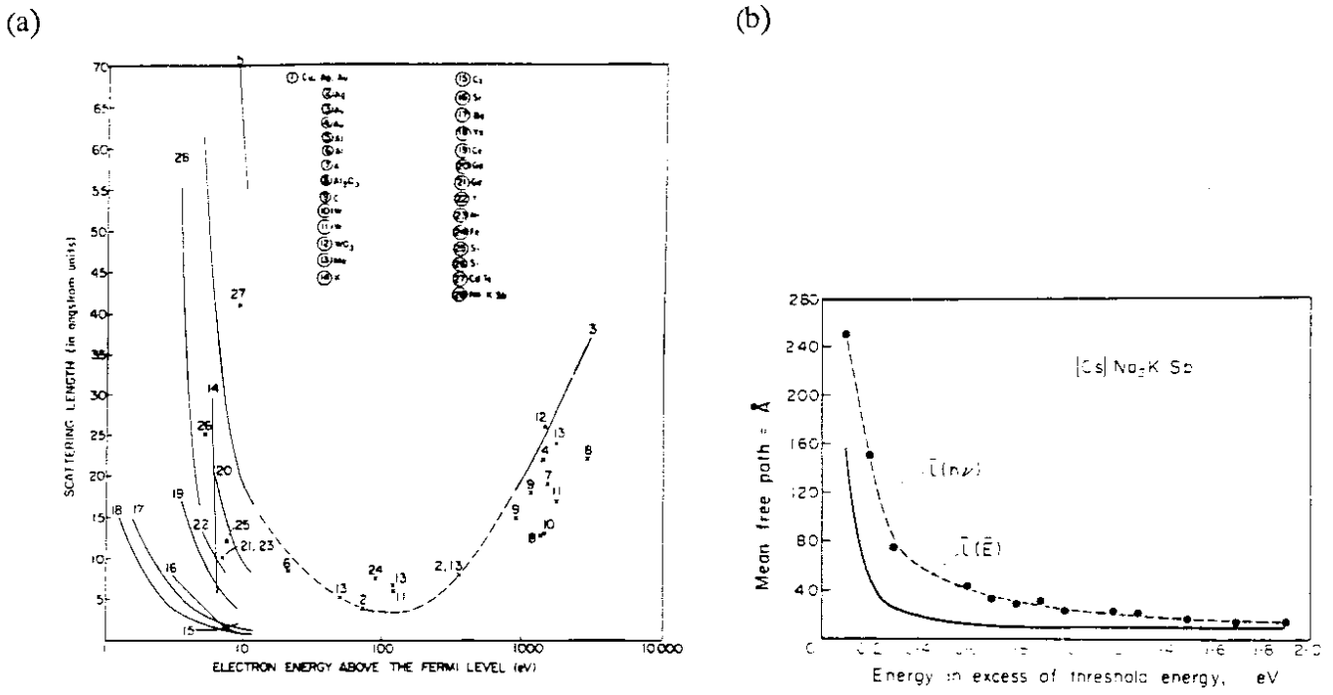

Figure 6. a) The escape depth is shown as a function of electron energy for a number of materials. b) Mean free path as a function of electron energy, $L(E)$, or photon energy, $L(h\nu)$, for the $[Cs]Na_2KSb$ cathode.

the electron must have an energy of at least E_g above the CBM in order to suffer electron-electron scattering. This is illustrated in Fig. 5. If the VL is low enough so that $E_A < E_g$, there is only electron-phonon scattering near threshold. A necessary condition for obtaining $L > l_a$ and high quantum efficiency is that electrons escape without suffering electron-electron scattering. This can only happen for nonmetals (semiconductors and insulators)—metals are never efficient photoemitters in the visible and near ultraviolet. Srong infrared or visible photoresponses are restricted to semiconductors (i.e., $E_g < 3$ eV).

In Fig. 5, we introduced the term "Magic Window" to indicate the energy region in which electrons can escape from the solid without electron-electron scattering. In Fig. 7 we show $L(h\nu)$ for a semiconductor with electron affinity $E_A < E_g$ and for a metal.

Summarizing this section, the requirement for an efficient emitter is that P_E and α_{PE}/α be large and l_a/L be small. This can be achieved by using a semiconductor with an electron affinity that is smaller than the band gap. The threshold for response is given by $E_g + E_A$ As A. H. Sommer emphasizes in his article in these proceedings [22], before 1965 all of the practical photocathodes were found by Edisonian research. It was for these cathodes (particularly the alkali-antimonides) that the theory given above was developed [7,13,14]. The negative affinity cathodes [23] were the first "scientifically engineered" photocathode. This has led to a new family of photocathodes [15,16,17,24,25]. The "scientific engineering" was based on the concepts contained in the theoretical framework of the Three–Step model.

Another important concept necessary to obtain this new family of photocathodes is that of lowering the electron affinity by band bending, which is illustrated in Fig. 8. This was developed independently by Spicer [7,14,26] and by Scheer and van Laar [27]. Once the importance of band bending was recognized in the context of the three step model, groups in several laboratories worked to develop a negative affinity cathode. Scheer and Van Laar were first to announce the practical development of a negative affinity photocathode, which was done using GaAs. The results were soon reproduced by Spicer group at Stanford (where he moved in 1962 from RCA Labs). Simon and Williams at RCA Labs independently developed a GaP negative affinity cathode; however, due to company policy, they were not able to announce it until 1968. Because of their growing importance, the next section will be devoted to a discussion of the negative affinity cathodes.

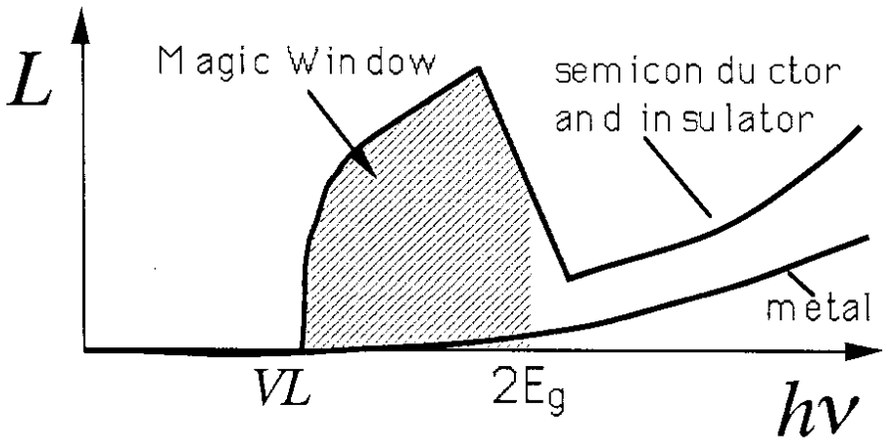

Figure 7. Average escape depth for metals and nonmetals. The "Magic Window" is the energy region defined by $VL < E < 2E_g$. Here the electrons have enough energy to escape but not to allow electron-electron scattering in the semiconductor.

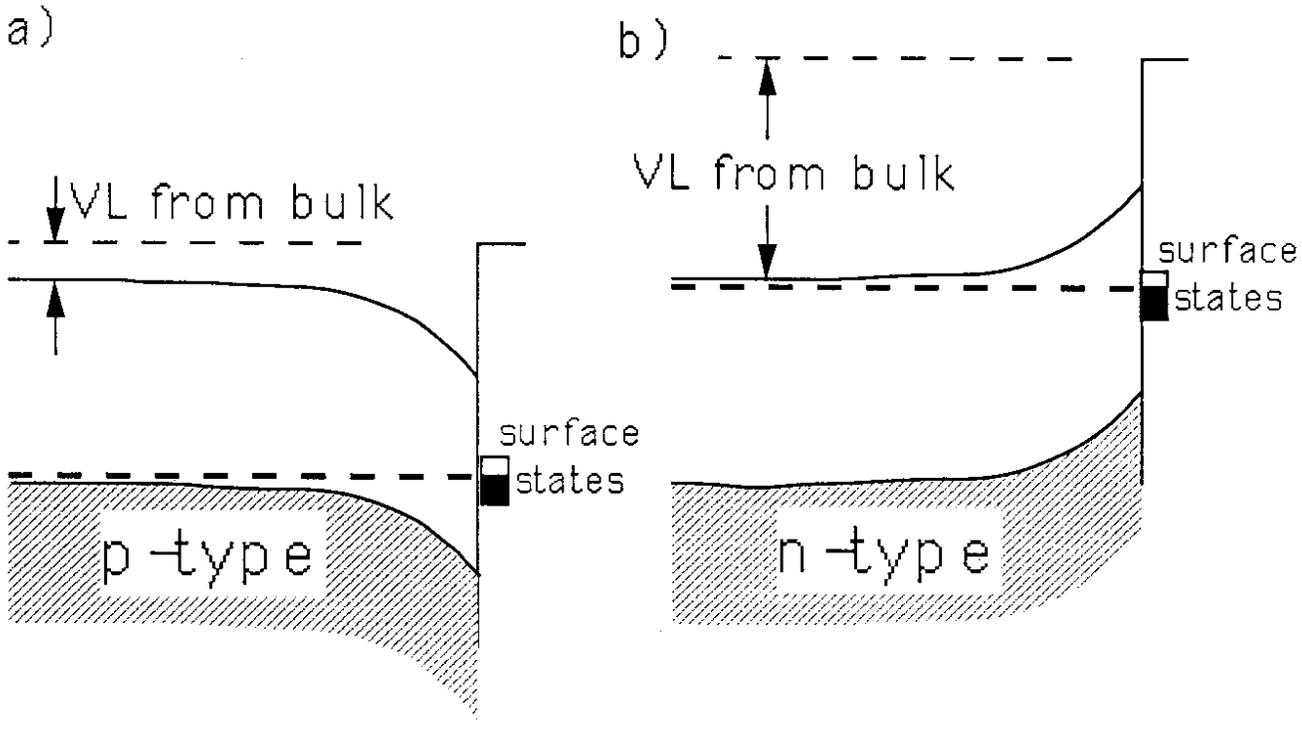

Figure 8. a) In p-type semiconductors the band bending is downwards, so the surface vacuum level decreases with respect to the bulk CBM, so the barrier seen by the electrons in the bulk is smaller than in the flat band case. b) For n-type, the band bending increases the barrier.

5. Negative Electron affinity Photocathodes

Figure 9 shows early results obtained by Eden and Spicer [31,32] just after Scheer and van Laar [23] announced their negative electron affinity cathode in 1965. In both the Stanford and Phillips cathodes, only Cs was used to reduce the electron affinity. Later it was found that Cs plus oxygen gave an even lower electron affinity and higher quantum yields. Most negative electron affinity (NEA) cathodes today are activated with Cs plus oxygen.

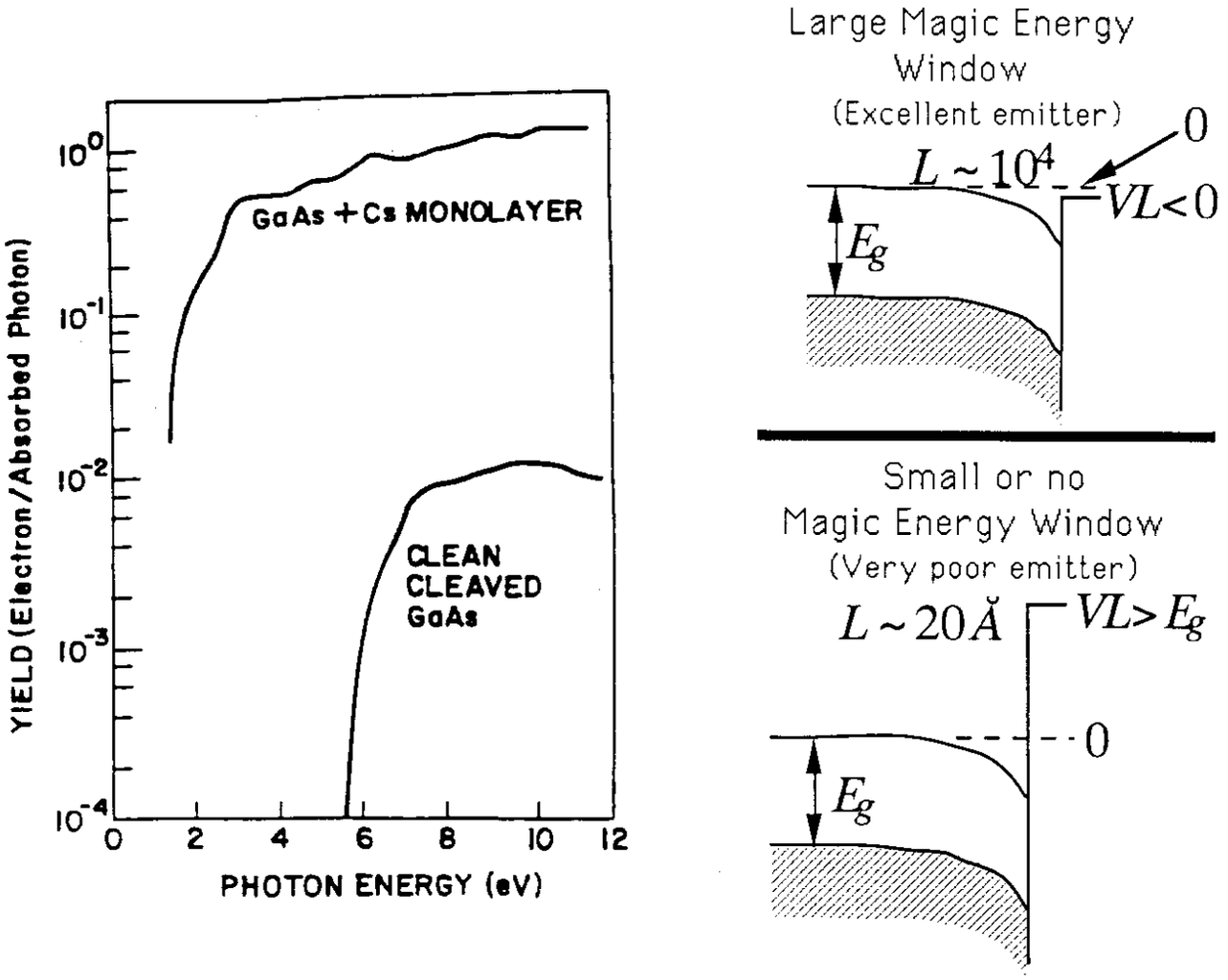

Figure 9. By the use of Cs, it is possible to decrease the surface Vacuum Level, improving the yield by orders of magnitude.

As the left-hand panel of Fig. 9 indicates, the yield without Cs is low and the threshold for response is well into the ultraviolet. With addition of a monolayer of Cs to the surface, the UV yield increases by 2 orders of magnitude and the threshold moves into the near infrared [33]. The right hand panels show the reason for this. With no Cs, the electron affinity is much larger (about 3.5 eV) than the band gap of 1.4 eV. For $h\nu$ near the threshold, $L(h\nu)$ is small, about 20Å and α_{PE}/α is also small. With addition of a Cs monolayer, the VL level is dropped below the bulk position of the conduction band minimum (CBM), thus the electron affinity takes on a negative value with respect to the bulk. Now α_{PE}/α is almost unity (it is not unity because there can always be some optical adsorption to states below the vacuum level in the band bending region; however, this will be quite small in the infrared and visible spectral regions). High doping ($10^{19}/cm^3$) is used in order to minimize the band bending region. Most importantly, $L(h\nu)$ is increased by almost 3 orders of magnitude. The large photoresponse of NEAs near threshold is due to the fact that electrons which are inelastically scattered may escape, even if they thermalize into the bottom of the conduction band.

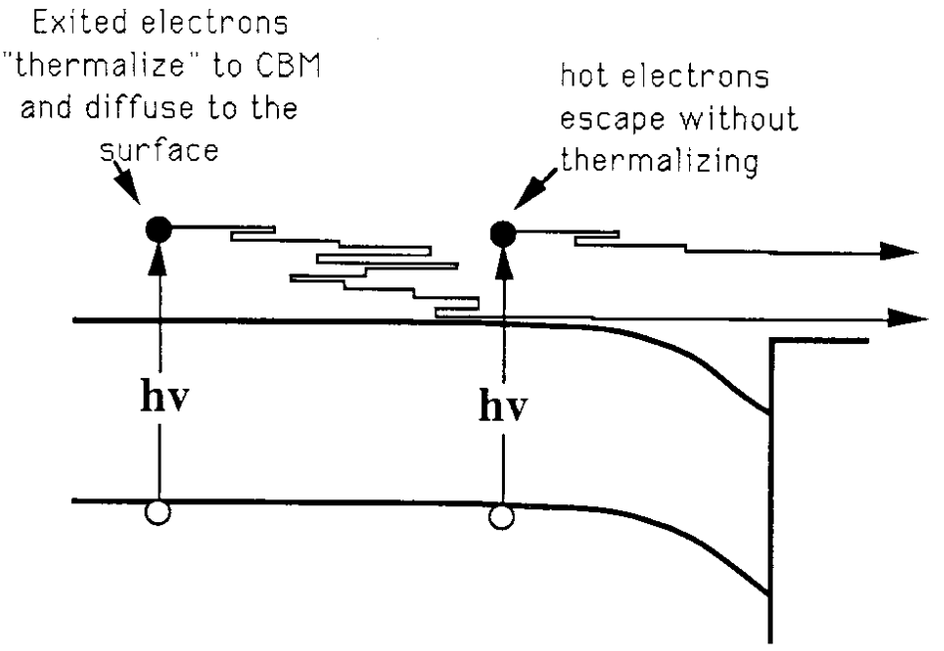

Figure 10. In the negative affinity cathodes, most of the electrons thermalize before escaping, although there is a fraction that escape without losing all their initial energy.

Figure 10 is a schematic diagram of the operation of a NEA cathode. For light excited deep in the semiconductor, the electrons will thermalize and diffuse to the surface. Despite the high doping, the diffusion length of the thermalized electron can be over 10^{-4} cm. Even for photons near the band gap, this is greater than the optical absorption depth (about 10^{-5} cm; thus, $l_a/L < 1$. As a result, the yield rises much more rapidly than for the older practical photocathodes near threshold.

The escape probability is found to be independent of $h\nu$ to a good approximation near threshold. This is to be expected since most electrons approaching the surface will have been thermalized into the CBM, so their energy does not depend on $h\nu$. Figure 11 shows values of P_E obtained by James and Bell [34] in 1972 for different GaAs crystal faces. P_E was found by fitting the experimental data to Eq. 8b; P_E is assumed to be independent of $h\nu$ above the photoemission threshold.

The value of L, obtained from the fit of the data of Fig. 11 to Spicer's Three–Step model, is about $6 \times 10^4 \mathring{A}$ (since l_a/L is so small, it is impossible to determine L very accurately). The values of P_E obtained from the fit are given in the right margin of Fig. 11. For practical cathodes, the (100) GaAs face is normally used because of the ease of preparation and the difficulty of reproducing the results of Fig. 9 in production facilities. After many years of experience with production of these cathodes, excellent tubes today have a value of P_E near 0.5.

Figure 12 gives the quantum yield curves for a group of cathodes made before 1978 [16]. A more recent yield results are presented at this meeting by a group from Intevac Inc. [24].

It has been possible to extend the threshold of these cathodes farther into the infrared ($\lambda < 2m$) by combining negative affinity approaches with structures that allow an internal potential to be applied across the semiconductor nearest the surfaces [16,17]. Further advances in these cathodes is presented by Intevac, Inc. in another paper in these proceedings [26].

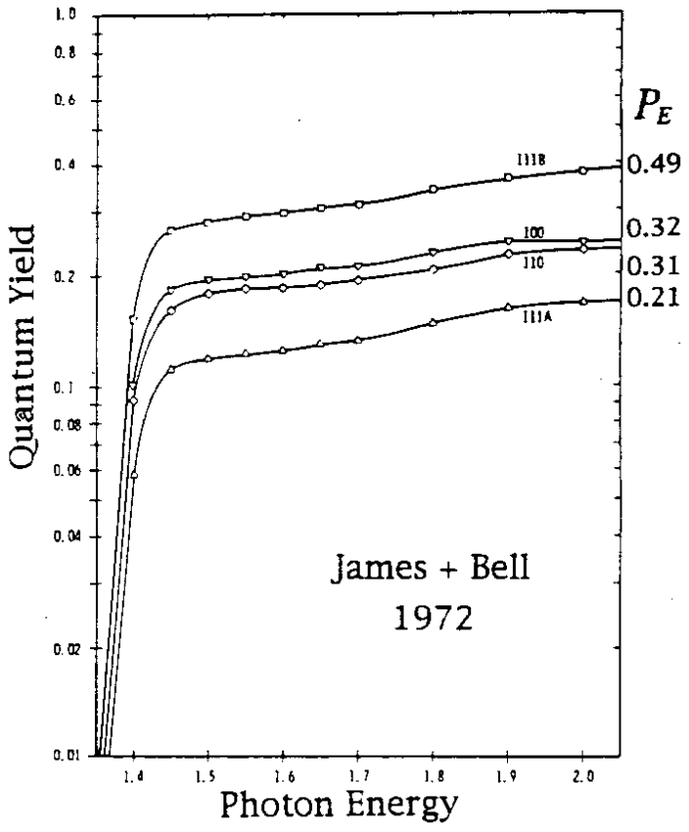

Figure 11. Dependence of the escape parameter, P_E, on crystal face for GaAs negative affinity photocathodes.

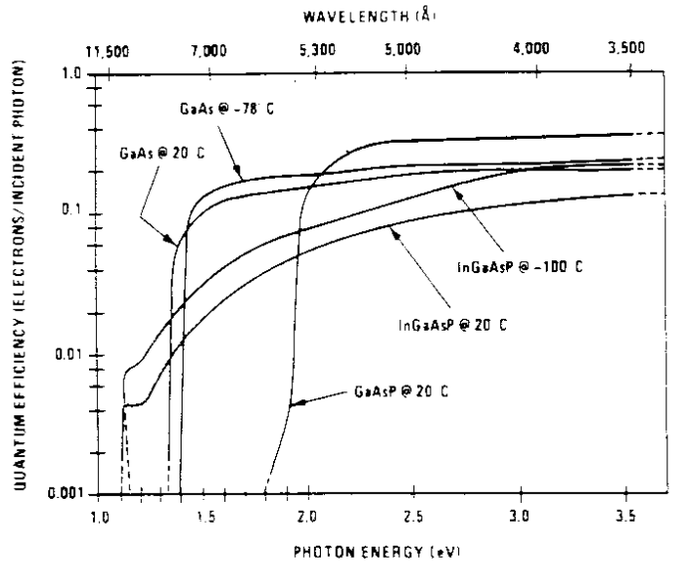

Figure 12. Quantum efficiency and threshold for NEA cathodes using different materials.

6. Requirements for High Frequency Phototubes

The first consideration for high-frequency phototubes is, of course, the response time of photoemission. This will be estimated here using the Three–Step model. A second consideration may be high current density, since this may be needed if a large amount of information is to be transmitted in a short period of time. This aspect will be considered by other papers in this meeting. The time response is determined by the time spread between photoexcitation and emission of the electrons into vacuum. Thus, the response time (τ) can be estimated as follows:

$$\tau = \int_0^{\tau} dt = \int_0^{L_T} \frac{dl}{v(l)} = \frac{\int_0^{L_T} dl}{v_a} = \frac{L_T}{v_a} , \tag{9}$$

where dl is an interval over the electron path length (L_T), $v(l)$ is the electron speed at the position l along the trajectory, and $v(a)$ is the average speed of the electron over its complete trajectory (see Fig. 4). The nature of the integrated path length depends on the scattering mechanisms, as discussed in Section 4.

Let us start by discussing the case where electron-electron scattering dominates (metals and semiconductors with $E_a > E_g$), where we can approximate L_T by the electron-electron scattering length L_e.

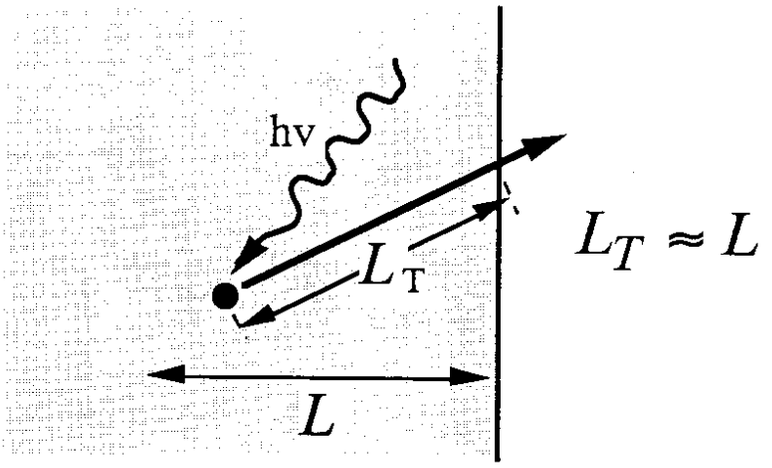

Figure 13. Trajectory of a photoemitted electron when the electron-electron scattering is dominant.

We calculate the response times for photon energies 1 eV above the threshold of response. We take the electron velocity given by a free electron relation and take the kinetic energy as zero at the Fermi energy for metals and at the conduction band minimum for semiconductors. For the metals mentioned above, $L \approx 40$ Å and the quantum yields varies from $8x10^{-5}$ to $4x10^{-4}$ as determined from the experiment [18], thus $\tau \approx 3x10^{-15}$. Allowing for uncertainties, we give a range of $10^{-15} \leq \tau \leq 10^{-14}$ sec. Materials such as clean Cu, Au, and Ag are used to produce very short electron pulses for Free Electron Lasers.

The second type of cathode is that in which electron-electron scattering is unimportant compared to electron-phonon (electron-lattice) scattering. For the reasons given in Section 4, the members of this class are semiconductors (and insulators) where the electron affinity is less than the band gap (see Fig. 5). Because the energy loss per scattering event is small (about the phonon energy, e.g., 0.01 to 0.1 eV), electrons can suffer many collisions without loosing a large energy (e.g. ,1 eV). As a result, the integrated path length before escape can be much larger than the region discussed first, where electron-electron scattering dominates.

As an example we will consider the case of Cs_3Sb, an important practical photocathode, which was studied extensively by Spicer in the late 1950 [7,12,27]. To calculate τ, one must estimate the average energy loss per collision (ΔE_p), the electron-phonon scattering length (l_p), and the distance from the surface at which the "average" electron is

excited. Both the scattering length and the average energy loss per collision, are temperature dependent. They depend on the phonon population (N_{ph}), which is given by the Bose-Einstein statistics as follows:

$$N_{ph} = \frac{1}{1+e^{E_{ph}/kT}} , \tag{10}$$

where E_{ph} is the energy of the associated phonon vibration mode, k is the Boltzman constant, and T is the temperature. Reasonable numbers for Cs_3Sb are $l_p = 50\text{Å}$ and $\Delta E_p = 0.01eV$. The electron affinity and band gap for Cs_3Sb are [7] $E_a = 0.45eV$ and $E_g = 1.6eV$. Let us assume that an electron is photoexcited to an energy E_k above the surface vacuum level. The number of collisions it can suffer before it has too little energy to escape into vacuum is given by

$$N = \frac{E_k}{\Delta E_p} . \tag{11}$$

The maximum integrated path length will be

$$\int_0^L dl = N l_p = \frac{E_k}{\Delta E_p} l_p , \tag{12}$$

and

$$\tau = \frac{E_k}{\Delta E_p} \frac{l_p}{v_a} . \tag{13}$$

Again we assume the electrons are excited 1 eV above the VL, and calculate the electron velocity as described above. For practical cathodes of this class take $l_p = 100\text{Å}$ and $\Delta E_P = 0.03eV$. This gives a value for 4×10^{-13} for τ. To account for uncertainties in these estimates, we take $10^{-13} < \tau < 10^{-12}$ sec. The yields for practical photocathodes of this class 1 eV above threshold lie between 0.05 and 0.25 electrons/photon.

The third and last class of photoemitters corresponds to negative affinity photocathodes (see Fig. 9), which have the longest response time. Here the threshold of response is the band edge, where the optical absorption coefficient becomes very small. Electrons will be excited all the way up to distances of the order of microns from the surface. These electrons thermalize into the bottom of the conduction band and diffuse thermally to the surface. Here, the response time is

$$\tau = \frac{L_D^2}{\mu kT/q} , \tag{14}$$

where L_D is the electron diffusion length, μ is the electron mobility, and q is the electron charge. For GaAs negative affinity cathodes, L_D might vary from 10^4 to 6×10^4, and thus $2 \times 10^{-4} < \tau < 7 \times 10^{-9}$ sec.

Table 1 and Figure 14 give theoretical estimates of response time, as well as the range of yields, for these materials. The range in response time is very large—over 6 orders of magnitude. The quantum yield increases by 3 or 4 orders of magnitude as the time response increases. Thus, a price must be paid for fast response time in terms of a decrease in quantum efficiency. This is due to the fact that the optical absorption takes places over a distance that is usually much larger than the electron scattering length. As a result, the electrons excited farther from the surface scatter many times and take much longer to escape than those near the surface. If only the small fraction of electrons excited near the surface can escape, the response time will be fast and the yield small. The surprising thing is the fast variation in the estimated response times. The limited experimental experience on response times is in general agreement with these estimates. These calculations are for specific materials and photon energies. Similar calculations may be made for photoemission from other materials.

Material	Dominating mode of scattering	Equation for τ	Estimate range of τ (sec)	Typical yield (el/photon) 1 eV above threshold
Metals	Electron-electron	$\tau \approx \frac{L}{v_a}$ (9)	10^{-15} to 10^{-14}	$8x10^{-5}$ to $4x10^{-4}$
Semiconductors and insulators (Cs3Sb or multialkali)	Electron-lattice	$\tau = \frac{E_k}{\Delta E_p}\frac{l_p}{v_a}$ (13)	10^{-13} to 10^{-12}	0.05 to 0.25
Negative affinity	Electron-lattice (thermal diffusion of electrons in CBM)	$\tau = \frac{L_D^2}{\mu kT/q}$ (14)	2×10^{-10} to 7×10^{-9}	0.1 to 0.6

Table 1. Expressions for the response time (τ), based on the Three–Step model, for the different classes of photoemitters, showing the range of values of τ and of the yield.

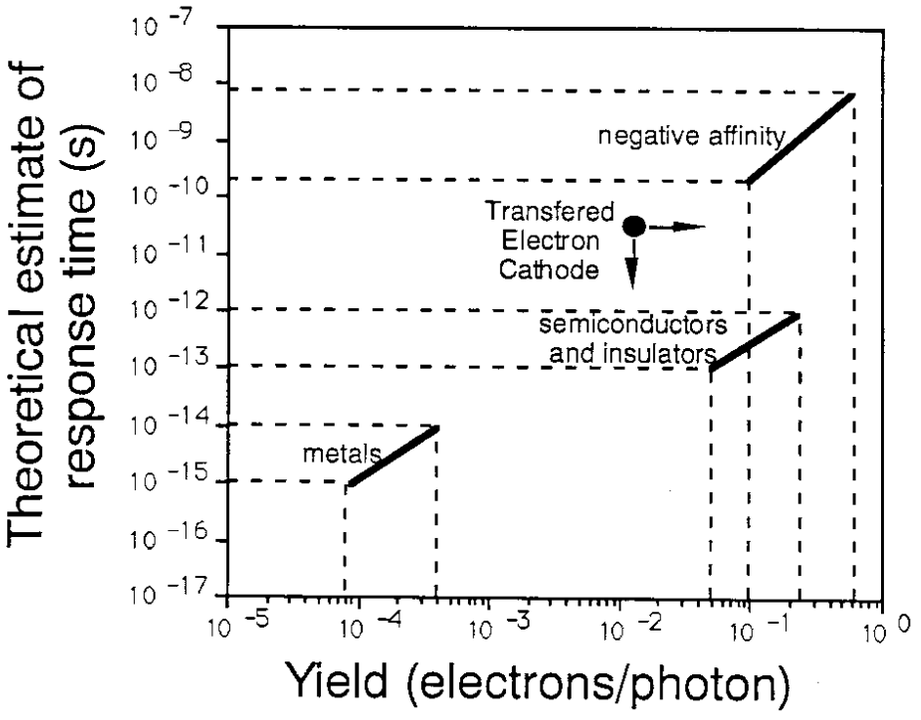

Figure 14. Range of values of τ from Table 1. The dot is for the Transferred Electron Cathode presented by Aebi et al. in these proceedings. The arrows on the dot indicate the directions in which improvements in performance are expected.

There is a way to speed up the escape of electrons from deeper in the material, by applying an internal electric field, which can accelerate them towards the surface [35,16]. Aebi et al. [26] will present results from such a structure (the Transferred Electron Cathode) in these proceedings. The point in Figure 14 refers to emission from a specific cathode with response near 1.4 μm. The time response for the Transferred Electron Cathode in Fig.14 was determined experimentally. Notice that it has a considerable faster time response with higher yield than the conventional photoemitters, as would be expected. As Aebi et al. [26] describe, it also has a longer wavelength response (about 1.4 μm) than the conventional cathode (see Fig. 12). Such cathodes, while complex to fabricate, give strong promise for the future if their usefulness justifies the expense of development and manufacture.

7. Other Requirements for New High Frequency Practical Devices

For brevity, only applications to high frequency devices have been mentioned. In addition to time response, two other requirements will be discussed: spectral sensitivity and the ability to produce high currents. Data on spectral responses for some existing photocathodes are available in this paper; others can be found in the literature (see, e.g., Ref. 13).

A potential use for fast photoemission devices is as fast receivers of signals from fiber optics. One potential benefit is the manipulation of electrons in vacuum by, for example, streak tubes to essentially increase the information handling capability of a receiving station. The problem is that the conventional cathodes do not have a long enough wavelength response to couple to fiber optics. For this reason, the Transferred Electron cathode described by Aebi et al. [26] was developed. This approach could be used to produce higher frequency response with increase yield at shorter wavelengths.

The second requirement is the drawing of high currents (even in short pulses) from photocathodes. This question must be examined for each class of photocathode. Papers by Alley et al. [36] and by Herrera-Gómez and Spicer [37] in these proceedings address this question in considerable detail. For the practical alkali-antimonide cathodes [13], special care must be taken. Because of their highly ionic nature, they tend to electrolyze if electric fields are developed across them, changing their properties. For both these materials and negative affinity materials, one must worry about the resistance of the cathode and be aware of the RC time constants which may limit their time response, even if the photoemission process does not limit it.

Metals, because of their high conductivity, are the simplest materials to consider, and are unlikely to have the problem outlined above. In general they also are least affected by less than ideal (10^{-10} Torr) vacuum. The price one pays is very small quantum yield.

8. Conclusions

The time response and quantum yield of photocathodes depend on the materials used. The established Three–Step model can be used to estimate the time response for various cathodes and to correlate this with the quantum yield. As expected from this theory, faster time response is associated with decreased yield (see Fig. 13). For very small yields (e.g., 10^{-4} electrons/photon) time responses of 10^{-15} to 10^{-14} sec can be expected. For materials which give very high yields (e.g., 0.3 electrons/photon) the time response can be 10^{-8} or longer. Both yields and time response are shown to depend on the scattering of the photoexcited electrons in the solid. For metals, the powerful electron-electron mechanism usually dominates, so that only electrons excited close to the surface can escape. This leads to the fastest response time and the lowest quantum yield. Semiconductors with small but positive electron affinities (see Fig. 5) have intermediate response times of order 10^{-13} to 10^{-12} sec and yields of 0.05 to 0.25 electrons per photon. The highest yields (0.1 to 0.6 electrons per photon) and longest response times are obtained from negative electron affinity photocathodes. The new Transferred Electron (field assisted) cathode gives faster response with quantum yield larger than the conventional cathodes. In addition, it has a longer wavelength (1.4 μm) response.

9. Acknowledgments

The help of Albert Green in critically reading this manuscript is gratefully acknowledged. This work was supported in part by Department of Energy contract DE-AC03-76SF00515 (SLAC/SSRL), and in part by the Dean of Engineering, Stanford University (W.E.S.) and by CONACyT-México (A.H.).

10. References

1) M. Cardona and L. Ley, eds. Photoemission in Solids I, Springer-Verlag, Berlin, Heidelberg, New York, 1978. G. Margaritondo, Physics Today, p. 66, 1988.
2) W.E. Spicer, "Photoemission from the past to the future," C. Coluzza, R. Sanjines, and G. Margaritondo, eds., Repro, Ecole Polytechnique Federale de Lousana, Switzerland, p. 1, 1992.
3) W.E. Spicer, "Chemistry and Physics of Solid Surfaces IV," R. Vanselaw and R. Howe, Springer-Verlag, Berlin, Heidelberg, p. 1, New York, 1982.
4) A.L. Hughes and L. A. Dubridge, Photoelectric Phenomena, McGraw-Hill, New York and London, 1932.
5) H.Y. Fan, Phys. Rev. Vol. 68, p. 43, 1945.
6) W.E. Spicer, "Amorphous and Liquid Semiconductors," Proceedings of the 5th International Conference, J. Stuke and W. Breniq, eds., Taylor and Francis Ltd,. p. 499, London, 1974.
7) W.E. Spicer, Phys. Rev. Vol. 112, p. 114, 1958.
8) The Oliver E. buckley Award of the Amer. Phys. Soc. was given to W.E. Spicer with D. Eastman in 1980, with the citation to W.E. Spicer, "For his effective development and application of photoemission spectroscopy as an indispensable tool for study of bulk and surface electronic structure of solids."
9) C.N. Berglund and W.E. Spicer, Phys. Rev. Vol. 4A, p. A1030 and 1044, 1964.
10) I. Lindau and W.E. Spicer, J. Electron. Spectrosc. Vol. 3, p. 409, 1974.
11) A.H. Sommer, Photoemissive Materials, Jonh Wiley and Sons, Inc., New York, Sidney, Toronto, 1968. Reprinted, Robert E. Krager Pub. Co., Huntington, New York, 1980.
12) W.E. Spicer, J. of Appl. Phys Vol. 34, p. 2077, 1960. W.E. Spicer and F. Wooten, Proc. IEEE Vol. 51, p. 1119, 1963.
13) R.L. Bell, Negative Electron Affinity Devices, Clarendon Press, Oxford, 1973. John S. Escher, "NEA Semiconductors Photoemitters," Semiconductors and Semimetals R.K. Willardson and A.C. Beer, Academic Press Inc., Boston, 1982.
14) T.H. Di Stefano and W.E. Spicer, Phys. Rev. B Vol. 7, p. 1554, 1973.
15) W.E. Spicer, Appl. Phys. Vol. 12, p. 115, 1977.
16) J.S. Escher, "NEA Semiconductors Photoemitters," Semiconductors and Semimetals Vol. 15, R.K. Willardson and A.C. Beer, Academic Press, Boston 1980.
17) W.E. Spicer, J. Phys. Chem. Solids Vol. 22, p. 365, 1961.
18) W.F. Krolicowski and W.E. Spicer, Phys. Rev. Vol. 185, p. 882, 1969. Phys. Rev. B Vol. 1, p. 478, 1970.
19) E.O. Kane, Phys. Rev. Vol. 159. p. 624, 1967.
20) R.N, Stuart, F. Wooten, and W.E. Spicer, Phys. Rev. Vol. 135, p. A495, 1964. R.N. Stuart and F. Wooten, Phys. Rev. Vol. 156, p. 799, 1966.
21) N.S. Smith and W.E. Spicer, Phys. Rev. Vol. 188, p. 593, 1969. N. S. Smith and G.B. fisher, Phys. Rev. B Vol 3, p. 3662, 1971.
22) Usually only the valence band contains high enough density of electrons to provide significant electron-electron scattering so as to have a major effect on photoemission.
23) A.H. Sommer, these proceedings.
24) J.J. Scheer and J. van Laar, Solid State Comm. Vol. 3, p. 189, 1965.
25) R.A. La Rue, J.P. Edgecomb, G.A. Davis, S.B. Gospe, and V.W. Aebi, these proceedings.
26) V.W. Aebi, K.A. Costello, G.A. Davis, and R. Weiss, these proceedings.
27) W.E. Spicer, R.C.A. Rev. Vol. 19, pp. 555–563, 1958.
28) J.J. Scheer and P. Zalm, Phillips Res. Repts. Vol. 14, pp. 143–50, 1959. J.J. Scheer, Phillips Res. Repts. Vol. 15, p. 584, 1960. J. van Laar and J.J. Scheer, Surface Science Vol 8, p. 342, 1967.
29) L.W. James, J.L. Moll, and W.E. Spicer, Proc. of 1968 Intern. Conf. on GaAs, Dallas Texas, Oct. 16–18. L.Wl James and J.L. Moll, Phys. Rev. Vol 183, p. 740, 1969.
30) R. Bell and W.S. Spicer, IEEE Proc. Vol. 58, p. 1788, 1970.
31) R.C. Eden, Ph.D. dissertation, Stanford University, 1967.
32) W.E. Spicer and R.C. Eden, Proc. of 9th Int. Conf. on Physics of Semiconductors Vol. 1, p. 65, Moscow 1968.
33) Due to the pioneering nature of this 1965-66 study, the infrared response is much less than that routinely obtained today. For example, only Cs was used in this activation, whereas the Cs and Oxigen process used today was developed a few yesrs later.
34) L.W. James, G.A. Antypas, J. Edgecumbe, R.L. Moon, and R.L. Bell, J. Appl. Phys. Vol 42, p. 4976, 1971.
35) R.E. Simon and W.E. Spicer, J. Appl. Phys. Vol. 31, p. 1505, 1960.
36) R.K. Alley, J. Clendening, C. Garden, E. Hoyt, R. Kirby, L. Kaisner, A. Kulikov, M. Woods, and D. Yeremian, these proceedings.
37) A. Herrera-Gómez and W.E. Spicer, these proceedings.